Journal Pre-proof

Influence of cation order on crystal structure and microwave dielectric properties in $x$$Li_{4/3}Ti_{5/3}O_4$-(1-$x$)$Mg_2TiO_4$ ($0.6 \leq x \leq 0.9$) spinel solid solutions

Lianting Nong, Xuefeng Cao, Chunchun Li, Laijun Liu, Liang Fang, Jibran Khaliq

PII: S0955-2219(21)00607-5

DOI: https://doi.org/10.1016/j.jeurceramsoc.2021.08.040

Reference: JECS 14283

To appear in: *Journal of the European Ceramic Society*

Received Date: 30 April 2021

Revised Date: 18 August 2021

Accepted Date: 19 August 2021

Please cite this article as: Nong L, Cao X, Li C, Liu L, Fang L, Khaliq J, Influence of cation order on crystal structure and microwave dielectric properties in $x$$Li_{4/3}Ti_{5/3}O_4$-(1-$x$)$Mg_2TiO_4$ ($0.6 \leq x \leq 0.9$) spinel solid solutions, *Journal of the European Ceramic Society* (2021), doi: https://doi.org/10.1016/j.jeurceramsoc.2021.08.040

Influence of cation order on crystal structure and microwave dielectric properties in $x$$Li_{4/3}Ti_{5/3}O_4$-(1-$x$)$Mg_2TiO_4$ ($0.6 \leq x \leq 0.9$) spinel solid solutions

Lianting Nong[1#], Xuefeng Cao[1#], Chunchun Li[1, 2, 3*], Laijun Liu[1], Liang Fang[1], Jibran Khaliq[3*]

[1]Guangxi universities key laboratory of non-ferrous metal oxide electronic functional materials and devices, College of Material Science and Engineering, Guilin University of Technology, Guilin, 541004, China

[2]School of Materials Science and Engineering, Nanchang University, Nanchang 330031, People's Republic of China

[3]Department of Mechanical and Construction Engineering, Faculty of Engineering and Environment, Northumbria University at Newcastle, NE1 8ST, UK

[#] These authors contribute equally.

[*] Authors to whom correspondence should be addressed: lichunchun2003@126.com; jibran.khaliq@northumbria.ac.uk

Abstract

Effect of order/disorder transition on microwave dielectric characteristics is reported to develop a deeper understanding of structure-property relationship in spinel ceramics. Dense $x$$Li_{4/3}Ti_{5/3}O_4$-(1-$x$)$Mg_2TiO_4$ ($0.6 \leq x \leq 0.9$) spinel ceramics were synthesized and characterized for structural and dielectric properties. The critical order/disorder structural transition was induced when $x < 0.8$, resulting in the ceramic crystallized into a primary cubic spinel phase, while when $x > 0.8$, the ceramic crystallized into a disordered face-centered cubic phase. The cation occupation caused this order-disorder transition, which directly influenced the variation in microwave dielectric properties. At $x = 0.75$ the maximum degree of order was achieved resulting in a maximum quality factor of 55,000 GHz and a near-zero τ_f = 2.9 ppm/^{o}C. Dielectric properties decreased sharply after $x = 0.8$ when the disorder face-centered cubic phase started to crystallize. All the results indicated that cation ordering/disordering plays a critical role in determining the optimum microwave dielectric properties in spinel ceramics.

Keywords: Ceramics; Dielectric materials; Microwave frequency; Cation order; Spinel

i. Introduction

In recent years, wireless communication systems have experienced enormous growth, leading to increasing demand for base materials such as microwave ceramics for applications in cell phones, radar, satellite broadcasting, and glob positioning systems [1-3]. Microwave dielectric ceramics are used to manufacture dielectric resonators, tubes, and microstrip lines, allowing microwave integration circuit (MIC) device sizes to be reduced to a millimeter scale. [2]. High quality factor ($Q\times f$) or low dielectric loss, feasible relative permittivity (ε_r, depending on application domains), and thermally stable operating frequency (τ_f) of microwave dielectric ceramics, make them the ideal candidate for MIC devices [4-8]. However, the three performance merits mentioned above tend to have a linear relationship among themselves to a certain extent (e.g., high-permittivity materials usually have high dielectric loss and large τ_f), and thus only limited microwave dielectric ceramics have been practically applied, including $CaTiO_3$-$MgTiO_3$, $(Zr, Sn)TiO_4$, $BaM'_{1/3}M''_{2/3}O_3$ (M′ = Zn, Mg, Co, Ni; M″ = Nb, Ta), and BaO-Ln_2O_3-TiO_2 tungsten bronzes, etc. [9-13] which suggests the need to explore new and innovative materials with optimised compositions to enhance the performance.

Recently, spinel oxides with a general formula of AB_2O_4 have been explored for microwave dielectric applications, mainly because of their extremely low dielectric losses (or high quality factors). For example, $MgAl_2O_4$ ceramics possess $Q\times f$~54,000 GHz [14] which is four-time higher than the $Ba_2ZnGe_2O_7$ ceramic [5]. In 2011, George et al. reported the notable dielectric performances of two Li-containing spinels $Li_2ATi_3O_8$ family (A = Zn, Mg), and their potential applications to succeed $(Zr, Sn)TiO_4$ [15]. Of particular interest are $Li_2MgTi_3O_8$, $Li_2Mg_3Ti_4O_{12}$, and $Li_4Ti_5O_{12}$ ceramics which belong to $xLi_{4/3}Ti_{5/3}O_4$-$(1-x)Mg_2TiO_4$ series and correspond to x = 0.5, 0.75, and 1, respectively. $Li_2MgTi_3O_8$ ceramics present a close-zero τ_f value of 3.2 ppm/°C along with ε_r = 27.2 and $Q\times f$ = 42,000

GHz. On the other hand, $Li_2Mg_3Ti_4O_{12}$ was reported to exhibit dielectric properties with $\varepsilon_r = 20.2$, $Q \times f$ = 62,300 GHz, and τ_f = -27.1 ppm/°C [16]. And $Li_4Ti_5O_{12}$ spinel demonstrates $\varepsilon_r \sim 30.1$, $Q \times f \sim 29{,}530$ GHz, and $\tau_f \sim$ -15 ppm/°C [17].

It is interesting to point out that the τ_f value follows a so-called sinewave which jumps from a negative value (-27.1 ppm/°C) at x = 0.5 to positive (3.2 ppm/°C) at x = 0.75, and bounces back to negative (-15 ppm/°C) at x = 1. Besides, both ε_r and $Q \times f$ also reveals obvious compositional dependence. Such a material system provides a sufficient platform to explore the relationship between composition, crystal structure, and physical properties. More importantly, at least two near-zero τ_f values are expected in the compositional spans x = 0.5 ~ 0.75 and x = 0.75 ~ 1 within this system.

In this paper, solid solutions of $x Li_{4/3}Ti_{5/3}O_4$-$(1-x)Mg_2TiO_4$ ($0.6 \leq x \leq 0.9$) system were synthesized to study the structure-properties relationship with composition change in order to achieve optimum set of properties and develop thermally stable microwave dielectric materials.

ii. Experimental procedures

In this work, a solid-state reaction route was applied to manufacture $x Li_{4/3}Ti_{5/3}O_4$-$(1-x)Mg_2TiO_4$ ($0.6 \leq x \leq 0.9$) ceramics using the reagent grade Li_2CO_3 (99.99%, Ltd Shanghai, China), TiO_2 (99.95%, Ltd Shanghai, China), and MgO (99.95%, Ltd Shanghai, China) powders. Stoichiometrically weighed raw materials were mixed in a ball mill using alcohol as a milling medium for 6 hours. After drying at 100 °C for 12 hours, the mixed powders were calcined at 900 °C for 6 hours, followed by a second ball milling to break the agglomerates using the same condition as above. Subsequently, the powders were dried and PVA was added as a binder and pressed into cylindrical disks with a diameter of 12 mm and 6-7 mm in height under a pressure of 150 MPa. The green disks were pre-heated at 550 °C for 6 h

to evaporate PVA and then sintered at temperatures ranging from 960-1180 °C for 6 h to densify the ceramics.

The bulk density was measured using Archimedes method and the phase purity was confirmed by X-ray diffraction (Cu*K*α1, 1.54059 A, Model X'Pert PRO, PANalytical, Almelo, The Netherlands). The microstructure was characterized on the polished and thermally etched surfaces (thermal etching temperature was 50 °C lower than the optimum sintering temperature) using a Scanning Electron Microscope (SEM; Model JSM6380–LV, JEOL, Tokyo, Japan). The room-temperature Raman spectra were collected using a Raman spectrometer (DXR; Thermo Fisher Scientific, American). The microwave dielectric properties were measured based on the Hakki-Coleman method using a network analyzer (Model N5230A, Agilent Co., Palo Alto, Canada) equipped with a temperature chamber (Delta 9039, Delta Design, San Diego, CA) [18]. The temperature coefficient of resonant frequency was calculated by the equation:

$$\tau_f = \frac{f_2 - f_1}{f_1(T_2 - T_1)} \times 10^6 (\text{ppm}/^\circ\text{C}) \qquad (1)$$

where f_1 and f_2 are the resonant frequency at T_1 (25 °C) and T_2 (85 °C), respectively.

iii Results and discussions

XRD patterns of $x\text{Li}_{4/3}\text{Ti}_{5/3}\text{O}_4$-$(1\text{-}x)\text{Mg}_2\text{TiO}_4$ ($0.6 \le x \le 0.9$) ceramics sintered at their respective densification temperatures for 6 h are shown in Fig. 1a. By indexing with the standard PDF card (No. 48-0263 for $\text{Li}_2\text{MgTi}_3\text{O}_8$ and No. 49-0207 for $\text{Li}_4\text{Ti}_5\text{O}_{12}$), the cubic spinel structure was confirmed. No other impurity phase was detected within the accuracy of XRD, indicating the phase purity for all compositions. $\text{Li}_4\text{Ti}_5\text{O}_{12}$ ($[\text{Li}]^{tet}[\text{Li}_{1/3}\text{Ti}_{5/3}]^{oct}\text{O}_4$) crystallizes into a cubic spinel structure with no prominent cation ordering on both the tetrahedral and octahedral sites, whereas $\text{Li}_2\text{MgTi}_3\text{O}_8$

($[LiMg]^{tet}[LiTi_3]^{oct}O_8$) has a special 1:3 cation ordering on the octahedral sites [19-21]. When $0.6 \leq x \leq 0.8$, the compositions tend to materialize the ordered spinel, similar to $Li_2MgTi_3O_8$ with a space group $P4_332$, whereas such compositions with $x > 0.8$ develop the disordered spinel, similar to $Li_4Ti_5O_{12}$ with a space group *Fd-3m*. Enlarged pattern of the main peak (311) positioned at $2\theta = 36$ ° are shown in Fig. 1b. It can be clearly seen that the (311) peak gradually shifted towards higher angle as x increased, indicating the solid solution formation and the lattice contraction [22-24]. In order to explore the cation ordering/disordering transition within the crystal structure, the strongest (311) peak was compared with the diffraction peaks of (110), (210), (211), and (310) in the $Li_2MTi_3O_8$ spinel phase as they reflect the cation ordering in the octahedral site [25] and are shown in Fig. 1c. With x increasing from 0.6 to 0.8, the relative intensity of these peaks increased initially reaching a maximum value at $x = 0.75$, followed by a decrease. This indicates that at $x = 0.75$ ($Li_2MgTi_3O_8$), the ceramic had the highest "ordering degree" within this $xLi_{4/3}Ti_{5/3}O_4$-$(1-x)Mg_2TiO_4$ system. These variations can be ascribed by the ordering of Li^+ and Ti^{4+} cation in the octahedral sites.

To further analyze the phase purity and composition, Rietveld refinement using Fullprof software was employed. The representative profiles are shown in Fig. 1d for $x = 0.6$ composition. As shown (Fig. 1d and Supplementary Fig. S1), the calculated pattern matched well with the experimental patterns, giving rise to the low difference profile. It should be noted that the structural models for $x = 0.6$ and 0.8 were based on the $Li_2MgTi_3O_8$ while the model for $x = 0.9$ was based on $Li_4Ti_5O_{12}$ to accommodate the ordering/disordering transition. Fig. 1e shows the variation of cell parameter and volume with increasing x (from 0.6 to 0.9), exhibiting a downward trend consistent with the lattice contraction, which suggests the formation of solid solution.

Fig. 2 shows the SEM images of $xLi_{4/3}Ti_{5/3}O_4$-$(1-x)Mg_2TiO_4$ ceramics sintered at their respective

densification temperatures. All samples exhibited fine microstructures with clear grain boundaries and well-developed grains (Figs. S2), which corresponds to their high relative densities. Figs. S3 (in the Supplementary Material) shows the densities for $x$$Li_{4/3}Ti_{5/3}O_4$-(1-$x$)$Mg_2TiO_4$ ceramics as a function of sintering temperatures. Sintering temperature of all the compositions were optimized to achieve a relative density higher than 93% as lower density negatively affects the dielectric properties. It was interesting to note that, the densification temperature gradually decreased from 1140 °C to 1020 °C when x increased from 0.6 to 0.9. As mentioned earlier, the ordering/disordering transition took place at x = 0.75, it can be estimated that the lower densification temperature was a result of ordering of the crystal structure. This decrease could be attributed to the lower densification temperature of $Li_4Ti_5O_{12}$ (925 °C) [17].

Because of higher sensitivity of Raman spectroscopy for ion/group vibration compared to XRD, Raman spectroscopy was employed to understand the ordering/disordering transition in the crystal structure of $x$$Li_{4/3}Ti_{5/3}O_4$-(1-$x$)$Mg_2TiO_4$. The room-temperature Raman spectra are shown in Fig. 3a and fitted via a Gaussian-Lorentzian function (Fig. S4) for various compositions. Obvious compositional dependence was discovered in the room-temperature Raman spectra, as characterized by the change in Raman intensity (Fig. 3b), peak width (Fig. 3c), and wavenumber (Fig. 3d). Upon increasing x from 0.6 to 0.9, the intensity increased initially and then decreased with a maximum value at x = 0.75 which is consistent with XRD results. With increasing x value, the peak at 718 cm^{-1} shifted towards a lower wavenumber while the peak at 400 cm^{-1} shifted towards a higher wavenumber. Some Raman modes (e.g., 450 cm^{-1}, 534 cm^{-1}, and 634 cm^{-1}) decreased their intensity and even vanished with increasing x value. Such variations stem from the difference in the cation distribution between ordered and disordered spinel, as verified through XRD analysis.

Fig. 4 shows the key performance merits (ε_r, $Q\times f$, and τ_f) as a function of composition (x value). Relative permittivity (ε_r) featured a noticeable increase from 22.3 at x = 0.6 to 27.1 at x = 0.75, then decreases to 24.6 at x = 0.9 (Fig 4a). Similarly, with increasing x value the quality factor initially goes up significantly before achieving a maximum value of 55,000 GHz at x = 0.75. Upon further increasing x to 0.9, the quality factor started to decrease reaching an extremely low value of 27,800 GHz. Of particular importance was the varying τ_f values, which jumped from a negative value of -11.2 ppm/^{o}C at x = 0.6 to a positive value of 2.9 ppm/^{o}C at x = 0.75. A further increase in the x value to 0.9 decreased the τ_f to a high negative value of -19.8. Due to the order/disorder transition at x = 0.75, two zero-τ_f regions were made possible when $0.7 \leq x \leq 0.75$ and $0.75 \leq x \leq 0.8$. Together with excellent quality factors ($Q\times f$ = 40,600-55,000 GHz) and moderate relative permittivities (ε_r = 26-27.2). These combinations of dielectric properties prove ideal for the application fields with specific needs for low dielectric loss and stable temperature stability, e.g., satellite communications, military radar, etc. [1].

It is well known that the extrinsic (e.g., phase purity and constitutions, bulk density, grain size and distribution, etc.) and intrinsic factors (including crystal structure, ionic polarizability, phonon vibration, packing fraction, etc.) determine the ultimate dielectric properties [26-29].

Raman spectroscopy provided another evidence to explain the dielectric properties variation as a function of composition. The blue shift of a certain Raman mode indicates a higher lattice vibration energy, which means a rigid structure and thus lower relative permittivity [30]. [31-34]. Such correlation is responsible for an opposite variation trend between the relative permittivity and Raman shift of $A_{1g(2)}$, as shown in Fig. 5(a). However, the deviation from such a variation tendency at x = 0.9 is mainly due to the lower relative density (Fig.5). The porosity-corrected permittivities were calculated via using the Bosman and Having's equation [35]:

$$\varepsilon_{\text{corr}} = \varepsilon_{\text{r}}(1 + 1.5p) \qquad (3)$$

where p is the fractional porosity. After correction, an incremental trend (as shown in Fig. 5a) is evident for the ε_{corr} values as a function of x value. Fig. 5(b) depicts the variation of $Q\times f$ value and FWHM of $A_{1g(2)}$ mode shift with increasing x value. The $Q\times f$ value decreased while FWHM of $A_{1g(2)}$ mode increased, with increasing x. The highest intensity magnitude and lowest FWHM of the $A_{1g(2)}$ mode at x = 0.75 meant the high ordering degree in the spinel structure, which led to lower dielectric loss.

Packing fraction (P. F) which is defined by the ratio of the total volume of packed ions to the unit volume [36-38] presents a similar variation trend with the quality factor, and reaches the highest value of 62.2% at x = 0.75 as shown in Fig. 5b. Besides, the degree of the order has long been thought to be the most important intrinsic factor influencing the Q value of microwave dielectric ceramics. P.K. Davies *et al.* investigated the relationship between microwave dielectric loss of complex perovskites $Ba(Zn_{1/3}Nb_{2/3})O_3$-$BaZrO_3$ and B-site cation ordering degree and established a positive correlation between them, that is, a higher cation order degree corresponds to a higher $Q\times f$ value [39].

A comparison has been drawn between the microwave dielectric properties of some spinel ceramics and $x$$Li_{4/3}Ti_{5/3}O_4$-(1-$x$)$Mg_2TiO_4$ (x = 0.75). It can be seen that all the ceramics have excellent microwave dielectric properties however, one way or another, the combination of these properties are not optimum for practical applications. For instance, titanates and gallates have higher quality factors compared to other ceramics, however, their sintering temperatures are relatively higher. Similarly, Li-based ceramics has a relatively lower sintering temperature but the τ_f values cannot meet the practical requirement ($|\tau_f| \leq 10$ ppm/°C). In this work, the $x$$Li_{4/3}Ti_{5/3}O_4$-(1-$x$)$Mg_2TiO_4$ (x = 0.75) ceramic has a similar permittivity and quality factor compared to other Li-based ceramics but the τ_f value is near-zero (τ_f = 2.9 ppm/°C) which makes it an excellent choice for practical applications.

iii. Conclusions

$x\mathrm{Li_{4/3}Ti_{5/3}O_4}$-$(1-x)\mathrm{Mg_2TiO_4}$ ($0.6 \leq x \leq 0.9$) spinel ceramics were synthesized using solid state reaction method and effect of composition induced order/disorder structure transition on microwave dielectric properties were studied. XRD and Raman analysis identified that compositions tend to crystallize in an ordered primary spinel ($x < 0.75$) while a disordered face-centered cubic structure was crystalized when $x > 0.75$. Therefore, $x = 0.75$ was the critical composition within the system at which the highest ordering degree took place A positive correlation between cation order and dielectric loss was established, as the highest quality factor ($Q \times f = 55{,}000$ GHz) was achieved at $x = 0.75$. Moreover, two zero regions of τ_f were observed between the composition range of $x = 0.65$ to 0.8 with lowest τ_f value of 2.9 being reported at $x = 0.75$ consistent with the composition with highest ordering degree. The findings presented in this paper not only add to our understanding of design philosophy for low-loss dielectric, but also make such spinels attractive candidates for dielectric resonances in microwave and millimeter-wave applications due to the combination of their thermal stability of resonance frequency, low relative permittivities, and high quality factors.

Conflict of interest statement

No conflict of interest exists in the submission of this manuscript, and the manuscript is approved by all authors for publication. I would like to declare on behalf of my co-authors that the work described was original research that has not been published previously, and is not under consideration

for publication elsewhere, in whole or in part.

Acknowledgments

Chunchun Li gratefully acknowledges the financial support from the Natural Science Foundation of China (No. 62061011), the Natural Science Foundation of Guangxi Zhuang Autonomous Region (No. 2018GXNSFAA281253, 2019GXNSFGA245006), and high-level innovation team and outstanding scholar program of Guangxi institutes, National Key Research and Development Plan of China (No. 2017YFB0406300).

References

[1] M.T. Sebastian, Dielectric materials for wireless communication, Elsevier Publishers, Oxford, U.K., 2008.

[2] M.T. Sebastian, H. Jantunen, Low loss dielectric materials for LTCC applications: a review, Int. Mater. Rev., 53 (2008) 57-90.

[3] R.V. Leite, F.O.S. Costa, M.T. Sebastian, A.J.M. Sales, A.S.B. Sombra, Experimental and numerical investigation of dielectric resonator antenna based on doped $Ba(Zn_{1/3}Ta_{2/3})O_3$ ceramic, J. Electromagnet. Wave, 33 (2019) 84-95.

[4] C.C. Li, H.C. Xiang, M.Y. Xu, Y. Tang, L. Fang, Li_2AGeO_4 (A = Zn, Mg): Two novel low-permittivity microwave dielectric ceramics with olivine structure, J. Eur. Ceram. Soc., 35 (2000) 2445-2456.

[5] C.C. Li, C.Z. Yin, J.Q. Chen, H.C. Xiang, Y. Tang, L. Fang, Crystal structure and dielectric properties of germanate melilites $Ba_2MGe_2O_7$ (M = Mg and Zn) with low permittivity, J. Eur. Ceram. Soc., 38 (2018) 5246-5251.

[6] D. Zhou, W.B. Li, H.H. Xi, L.X. Pang, G.S. Pang, Phase composition, crystal structure, infrared reflectivity and microwave dielectric properties of temperature stable composite ceramics (scheelite and zircon-type) in $BiVO_4$-YVO_4 system, J. Mater. Chem. C, 3 (2015) 2582-2588.

[7] Y. Wang, R.Z. Zuo, C. Zhang, J. Zhang, T.W. Zhang, Low-temperature-fired $ReVO_4$ (Re = La, Ce) microwave dielectric ceramics, J. Am. Ceram. Soc., 98 (2015) 1-4.

[8] C.C. Li, C.Z. Yin, M. Deng, L.L. Shu J. Khaliq, Tunable microwave dielectric properties in SrO-V2O5 system through compositional modulation, J. Am. Ceram. Soc., 103 (2020) 2315– 2321.

[9] L. Li, X.M. Chen, X.C. Fan, Microwave dielectric characteristics of $MgTiO_3$/$CaTiO_3$ layered ceramics, J. Electroceram., 15 (2005) 209-214.

[10] D.M. Iddles, A.J. Bell, A.J. Moulson, Relationships between dopants, microstructure and the microwave dielectric properties of ZrO_2-TiO_2-SnO_2 ceramics, J. Mater. Sci., 27 (1992) 6303-6310.

[11] D.M. Barber, K.M. Moulding, J. Zhou, M.Q. Li, Structural order in Ba $(Zn_{1/3}Ta_{2/3})O_3$, $Ba(Zn_{1/3}Nb_{2/3})O_3$, and Ba $(Mg_{1/3}Ta_{2/3})O_3$ microwave dielectric ceramics, J. Mater. Sci., 32 (1997) 1531-1544.

[12] M. Li, A. Feteira, M. Mirsaneh, M.T. Lanagan, D.C. Sinclair, A link between p-type electrical conduction and microwave dielectric loss in highly ordered $Ba(Co_{1/3}Nb_{2/3})O_3$ ceramics, J. Mater. Res., 25 (2010) 1011-1014.

[13] H. Zheng, I.M. Reaney, D. Muir, T. Price, D.M. Iddles, Effect of glass additions on the sintering and microwave properties of composite dielectric ceramics based on BaO-Ln_2O_3-TiO_2 (Ln = Nd, La), J. Eur. Ceram. Soc., 27 (2007) 4479-4487.

[14] P. Fu, W.Z. Lu, W. Lei, Y. Xu, X.H. Wang, J.M. Wu, Transparent polycrystalline $MgAl_2O_4$ ceramic fabricated by spark plasma sintering: Microwave dielectric and optical properties, Ceram. Int., 39 (2013) 2481-2487.

[15] S. George, M.T. Sebastian, Synthesis and microwave dielectric properties of novel temperature stable high Q, $Li_2ATi_3O_8$ (A = Mg, Zn) ceramics, J. Am. Ceram. Soc., 93 (2010) 2164-2166.

[16] H.F. Zhou, X.B. Liu, X.L. Chen, L. Fang, Preparation, phase structure and microwave dielectric properties of a new low cost $MgLi_{2/3}Ti_{4/3}O_4$ compound, Mater. Chem. Phys., 137 (2012) 22-25.

[17] H.F. Zhou, J.Z. Gong, N. Wang, X.L. Chen, A novel temperature stable microwave dielectric ceramic with low sintering temperature and high quality factor, Ceram. Int., 42 (2016) 8822-8825.

[18] B.W. Hakki, P.D. Coleman, A dielectric resonant method of measuring inductive capacitance in the millimeter range, IEEE Trans Microw Theory Tech, 8 (1960) 401-410.

[19] A. Navrotsky, O.J. Kleppa, The thermodynamics of cation distributions in simple spinels, J. Inorg. Nucl. Chem., 29 (1967) 2701-2714.

[20] W. Li, L. Fang, Y. Tang, Y.H. Sun, C.C. Li, Microwave dielectric properties in the $Li_{4+x}Ti_5O_{12}$ ($0 \leq x \leq 1.2$) ceramics, J. Alloys Compd., 701 (2017) 295-300.

[21] H. Kawai, M. Tabuchi, M. Nagata, H. Tukamoto, A.R. West, Crystal chemistry and physical properties of complex lithium spinels $Li_2MM'_3O_8$ (M = Mg, Co, Ni, Zn; M′ = Ti, Ge), J. Mater. Chem., 8 (1998) 1273-1280.

[22] C.Z. Yin, Z.Z. Yu, L.L. Shu, L.J. Liu, Y. Chen, C.C. Li, A low-firing melilite ceramic $Ba_2CuGe_2O_7$ and compositional modulation on microwave dielectric properties through Mg substitution, J. Adv. Ceram., 10 (2021) 108-119.

[23] F.Y. Huang, H. Su, Y.X. Li, H.W. Zhang, X.L. Tang, Low-temperature sintering and microwave dielectric properties of $CaMg_{1-x}Li_{2x}Si_2O_6$ (x = 0−0.3) ceramics, J. Adv. Ceram., 9 (2020) 471-480.

[24] K. Du, X.Q. Song, J. Li, J.M. Wu, W.Z. Lu, X.C. Wang, W. Lei, Optimised phase compositions and improved microwave dielectric properties based on calcium tin silicates, J. Eur. Ceram. Soc., 39 (2019) 340-345.

[25] I.A. Leonidov, O.N. Leonidova, R.F. Samigullina, M.V. Patrakeev, Structural aspects of lithium transfer in solid electrolytes $Li_{2x}Zn_{2-3x}Ti_{1+x}O_4$ ($0.33 \leq x \leq 0.67$), J. Struct. Chem., 45 (2004) 262-268.

[26] W. Li, J.H. Li, J.X. Shen, Y. Xu, Z.Z. Wang, X.B. Jia, Q.L. Pang, H.C. Guo, Crystal structure, Raman spectra, and microwave dielectric properties of high-Q $Li_2ZnTi_3O_8$ systems with Nb_2O_5 addition, Ceram. Int., 47 (2021) 8601-8609.

[27] C.Z. Yin, H.C. Xiang, C.C. Li, H. Porwal, L. Fang, Low-temperature sintering and thermal stability of Li_2GeO_3-based microwave dielectric ceramics with low permittivity, J. Am. Ceram. Soc., 101 (2018) 4608-4614.

[28] E.S. Kim, B.S. Chun, K.H. Yoon, Dielectric properties of $[Ca_{1-x}(Li_{1/2}Nd_{1/2})_x]_{1-y}Zn_yTiO_3$ ceramics at microwave frequencies, Mater. Sci. Eng.: B, 99 (2003) 93-97.

[29] C.Z. Yin, C.C. Li, G.J. Yang, L. Fang, Y.H. Yuan, L.L. Shu, J. Khaliq, $NaCa_4V_5O_{17}$: A low-firing microwave dielectric ceramic with low permittivity and chemical compatibility with silver for LTCC applications, J. Eur. Ceram. Soc., 40 (2020) 386-390.

[30] K. Xiao, Y. Tang, Y.F. Tian, C.C. Li, L. Duan, L. Fang, Enhancement of the cation order and the microwave dielectric properties of $Li_2ZnTi_3O_8$ through composition modulation, J. Eur. Ceram. Soc., 39 (2019) 3064-3069.

[31] P.K. Davies, J. Tong, T. Negas, Effect of ordering-induced domain boundaries on low-loss $Ba(Zn_{1/3}Ta_{2/3})O_3$-$BaZrO_3$ perovskite microwave dielectrics, J. Am. Ceram. Soc., 80 (1997) 1727-1740.

[32] J. Zhang, R.Z. Zuo, Effect of ordering on the microwave dielectric properties of spinel-structured $(Zn_{1-x}(Li_{2/3}Ti_{1/3})_x)_2TiO_4$ ceramics, J. Am. Ceram. Soc., 99 (2016) 3343-3349.

[33] C.J. Pei, J.J. Tan, Y. Li, G.G. Yao, Y.M. Jia, Z.Y. Ren, P. Liu, H.W. Zhang, Effect of Sb-site nonstoichiometry on the structure and microwave dielectric properties of $Li_3Mg_2Sb_{1-x}O_6$ ceramics, J. Adv. Ceram., 9 (2020) 588-594.

[34] H.C. Xiang, C.C. Li, H. Jantunen, L. Fang, A.E. Hill, Ultralow Loss $CaMgGeO_4$ Microwave Dielectric Ceramic and Its Chemical Compatibility with Silver Electrodes for Low-Temperature Cofired Ceramic Applications, ACS Sustain. Chem. Eng., 6 (2018) 6458-6466.

[35] S.H. Yoon, D.W. Kim, S.Y. Cho, K.S. Hong, Investigation of the relations between structure and microwave dielectric properties of divalent metal tungstate compounds, J. Eur. Ceram. Soc., 26 (2006) 2051-2054.

[36] S.H. Yoon, D. Kim, S. Cho, K.S. Hong, Investigation of the relations between structure and microwave dielectric properties of divalent metal tungstate compounds, J. Eur. Ceram. Soc., 26 (2006) 2051-2054.

[37] Q.W. Liao, L.X. Li, R. Xiang, D. Xiang, New Low-loss microwave dielectric material $ZnTiNb_2O_8$, J. Am. Ceram. Soc., 94 (2011) 3237-3240.

[38] E.S. Kim, B.S. Chun, R. Freer, R.J. Cernik, Effects of packing fraction and bond valence on microwave dielectric properties of $A^{2+}B^{6+}O_4$ (A^{2+}: Ca, Pb, Ba; B^{6+}: Mo, W) ceramics, J. Eur. Ceram. Soc., 30 (2010) 1731-1736.

[39] M. Xiao, Q.Q. Gu, Z.Q. Zhou, P. Zhang, Study of the microwave dielectric properties of $(La_{1-x}Sm_x)NbO_4$ (x = 0-0.10) ceramics via bond valence and packing fraction, J. Am. Ceram. Soc., 100 (2017) 3952-3960.

[40] A. Belous, O. Ovchar, D. Durilin, M.M. Krzmanc, M Valant, D. Suvorov, High-Q Microwave Dielectric Materials Based on the Spinel Mg_2TiO_4, J. Am. Ceram. Soc., 89 (2006) 3441-3445.

[41] S.P. Wu, J.J. Xue, R. Wang, J.H. Li, Synthesis, characterization and microwave dielectric properties of spinel $MgGa_2O_4$ ceramic materials, J. Alloys Compd., 585 (2014) 542-548.

[42] J.J. Xue, S.P. Wu, J.H. Li, Synthesis, Microstructure, and Microwave Dielectric Properties of Spinel $ZnGa_2O_4$

Ceramics, J. Am. Ceram. Soc., 96 (2013) 2481-2485.

[43] H.C. Xiang, L. Fang, W.S. Fang, Y. Tang, C.C. Li, A novel low-firing microwave dielectric ceramic $Li_2ZnGe_3O_8$ with cubic spinel structure, J. Eur. Ceram. Soc., 37 (2017) 625-629.

[44] H.F. Zhou, X.B. Liu, X.L. Chen, L. Fang, Y.L. Wang, $ZnLi_{2/3}Ti_{4/3}O_4$: A new low loss spinel microwave dielectric ceramic, J. Eur. Ceram. Soc., 32 (2012) 261-265.

[45] Q. Ma, S.P. Wu, Y.X. Fan, Synthesis and microwave dielectric properties of Zn_2SnO_4 ceramics, Ceram. Int., 40 (2014) 1073-1080.

[46] S. George, M.T. Sebastian, Synthesis and Microwave Dielectric Properties of Novel Temperature Stable High Q, $Li_2ATi_3O_8$ (A = Mg, Zn) Ceramics, J. Am. Ceram. Soc., 93 (2010) 2164-2166.

[47] L. Fang, D.J. Chu, H.F. Zhou, X.L. Chen, Z. Yang, Microwave dielectric properties and low temperature sintering behavior of $Li_2CoTi_3O_8$ ceramic, J. Alloys Compd., 509 (2011) 1880-1884.

[48] S.K. Singh, S.R. Kiran, V.R.K. Murthy, Structural, Raman spectroscopic and microwave dielectric studies on spinel $Li_2Zn_{(1-x)}Ni_xTi_3O_8$ compounds, Mater. Chem. Phys., 141 (2013) 822-827.

Figure captions

Figure 1 (a) XRD patterns for $x$$Li_{4/3}Ti_{5/3}O_4$-(1-$x$)$Mg_2TiO_4$ ($0.6 \leq x \leq 0.9$) sintered at their densification temperatures for 6 h in air; (b) the enlarge profile of (311) peak; (c) the integrated relative intensity of the superlattice reflections (110), (210), (211), and (310); (d) Rietveld refinement plots for x = 0.6; (e) variations in the lattice parameters as a function of x values.

Figure 2 SEM images for $x$$Li_{4/3}Ti_{5/3}O_4$-(1-$x$)$Mg_2TiO_4$ sintered at: (a) 1140 ^oC (b) 1060 ^oC (c) 1080 ^oC and (d) 1020 ^oC

Figure 3 (a) Raman spectra for $x$$Li_{4/3}Ti_{5/3}O_4$-(1-$x$)$Mg_2TiO_4$; (b) variations in the Raman intensity; (c) variations in the FWHM, and (d); variations in the Raman shift for the $A_{1g(1)}$ and $A_{1g(2)}$modes

Figure 4 Microwave dielectric properties for $x$$Li_{4/3}Ti_{5/3}O_4$-(1-$x$)$Mg_2TiO_4$ as a function of x value; (a) ε_r; (b) $Q\times f$, and; (c) τ_f

Figure 5 (a) the variation of relative permittivity and Raman shift of $A_{1g(2)}$ mode and; (b) the quality factor ($Q\times f$), packing fraction, and FWHM of $A_{1g(2)}$ mode.

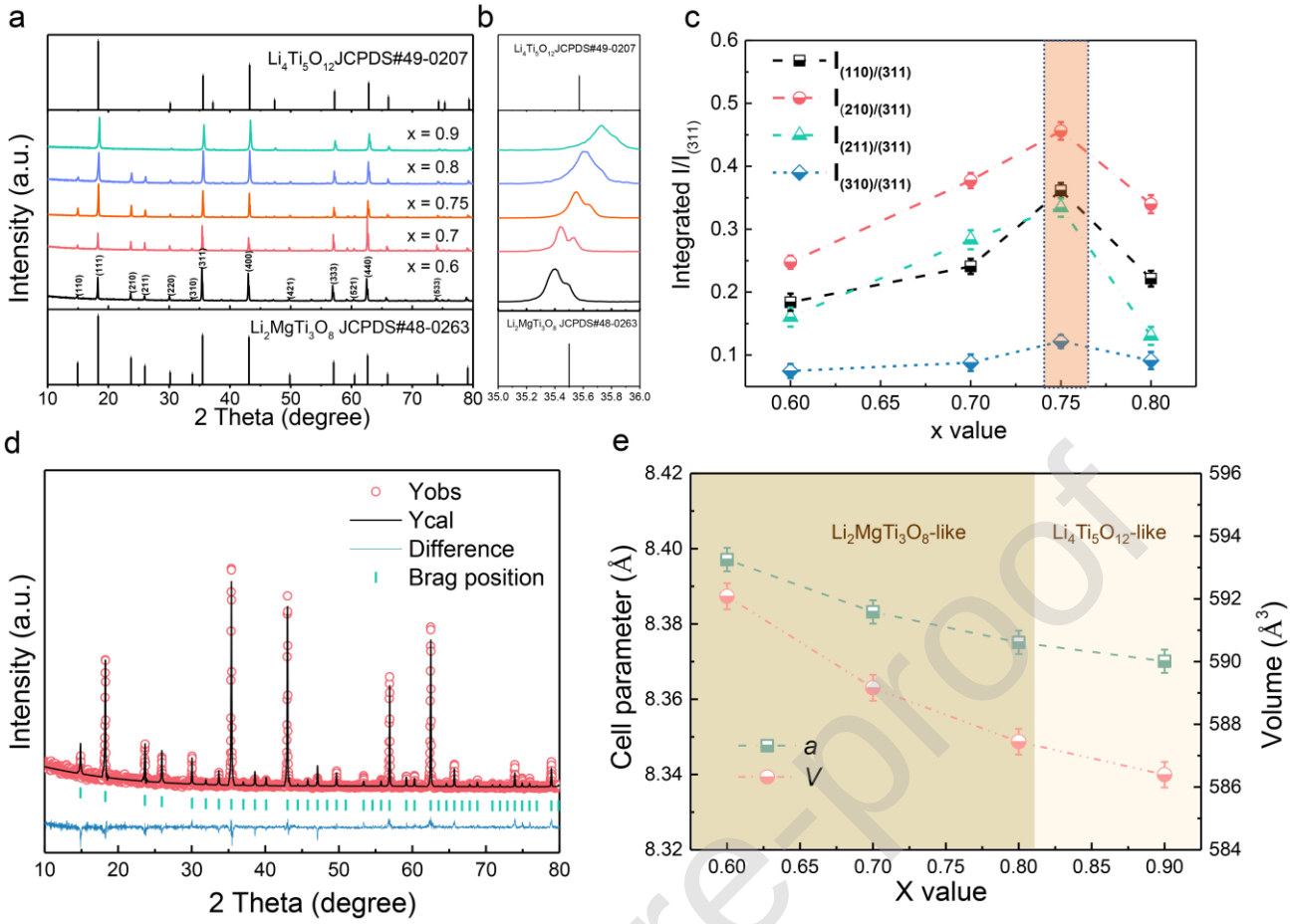

Figure 1 (a) XRD patterns for $xLi_{4/3}Ti_{5/3}O_4$-$(1-x)Mg_2TiO_4$ ($0.6 \le x \le 0.9$) sintered at their densification temperatures for 6 h in air; (b) the enlarge profile of (311) peak; (c) the integrated relative intensity of the superlattice reflections (110), (210), (211), and (310); (d) Rietveld refinement plots for x = 0.6; (e) variations in the lattice parameters as a function of x values.

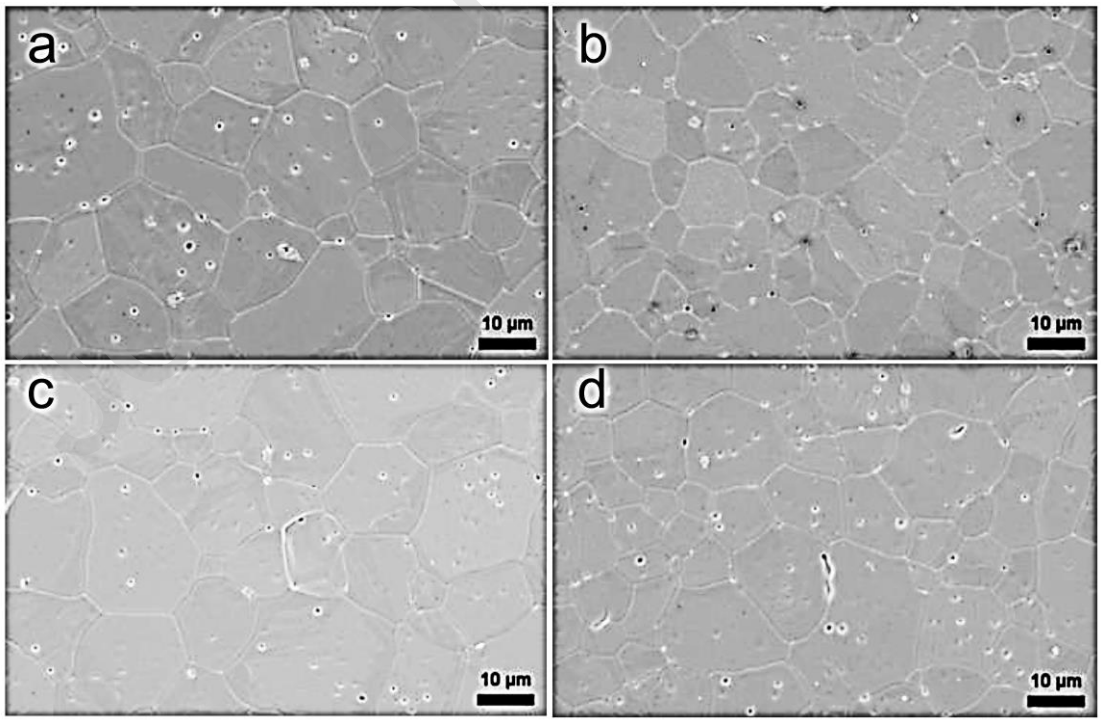

Figure 2 SEM images for xLi$_{4/3}$Ti$_{5/3}$O$_4$-(1-x)Mg$_2$TiO$_4$ sintered at: (a) 1140 ^{o}C (b) 1060 ^{o}C (c) 1080 ^{o}C and (d) 1020 ^{o}C

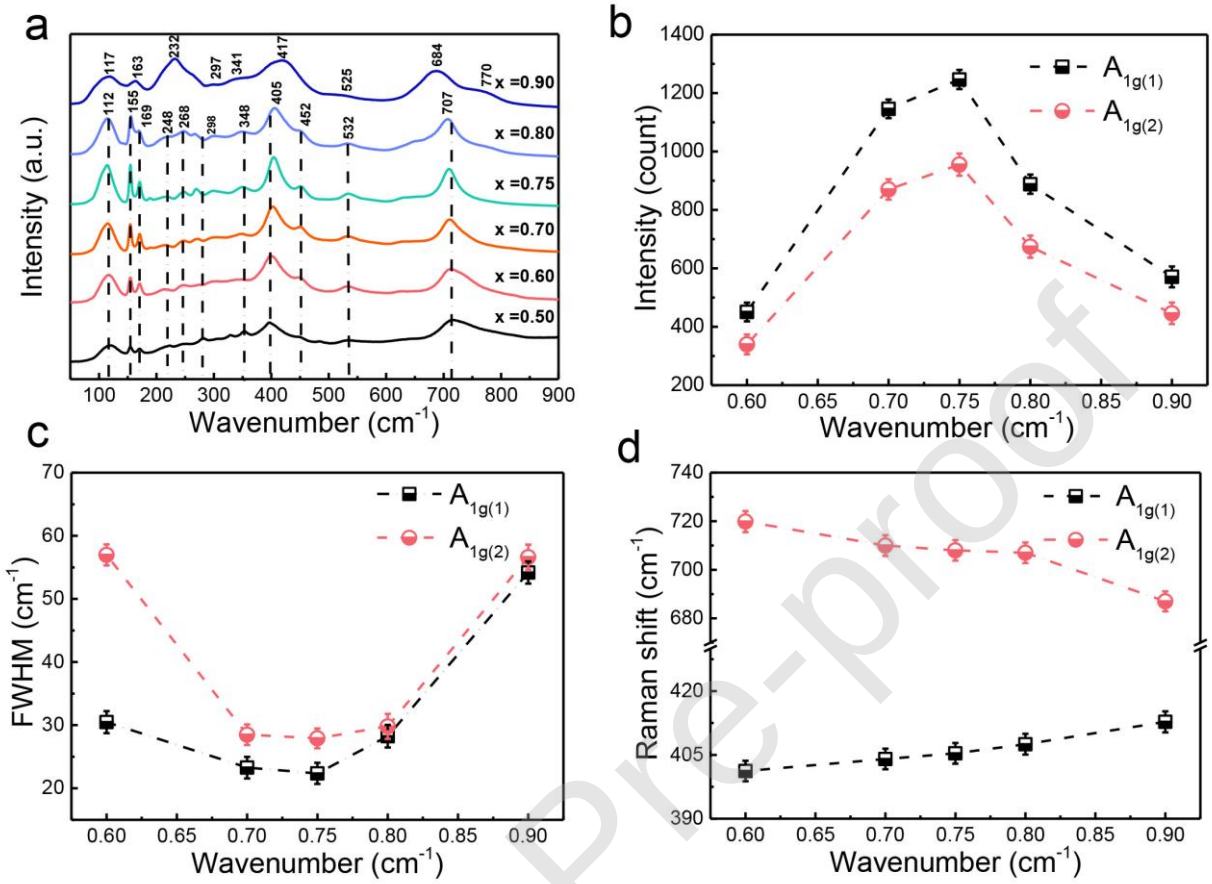

Figure 3 (a) Raman spectra for xLi$_{4/3}$Ti$_{5/3}$O$_4$-(1-x)Mg$_2$TiO$_4$; (b) variations in the Raman intensity; (c) variations in the FWHM, and (d); variations in the Raman shift for the $A_{1g(1)}$ and $A_{1g(2)}$modes.

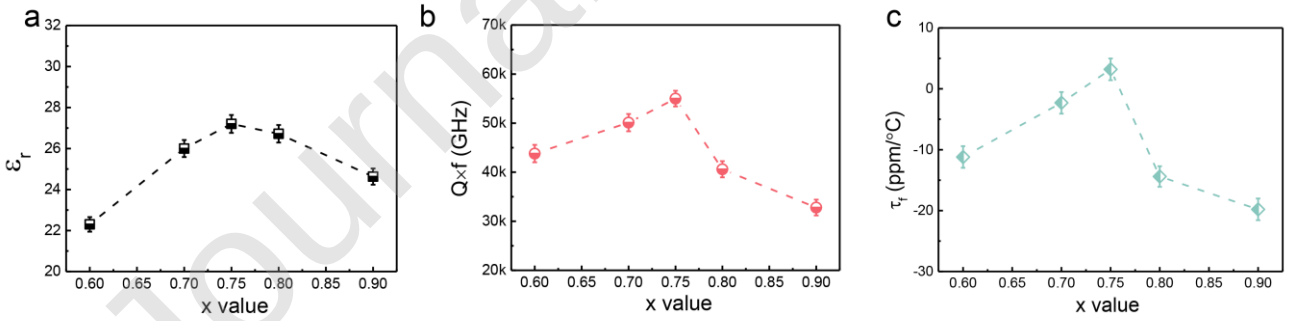

Figure 4 Microwave dielectric properties for xLi$_{4/3}$Ti$_{5/3}$O$_4$-(1-x)Mg$_2$TiO$_4$ as a function of x value; (a) ε_r; (b) $Q\times f$, and; (c) τ_f

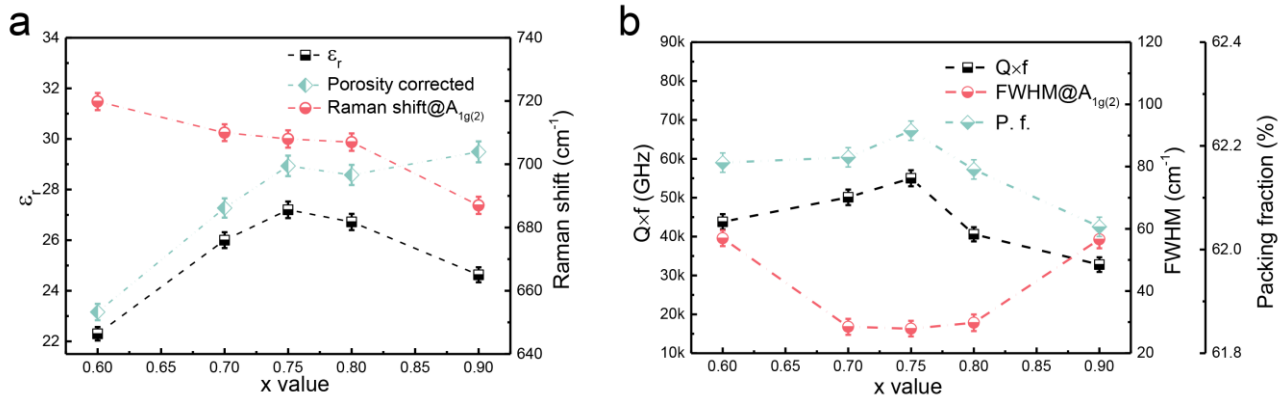

Figure 5 (a) the variation of relative permittivity and Raman shift of $A_{1g(2)}$ mode and; (b) the quality factor (*Q*×*f*), packing fraction, and FWHM of $A_{1g(2)}$ mode.

Table 1 Sintering temperature and microwave dielectric properties of some spinel structured ceramics

Ceramic	Sintering Temperature (°C)	Microwave dielectric properties			Reference
		ε_r	$Q\times f$ (GHz)	τ_f (ppm/°C)	
Mg_2TiO_4	1450	14	150,000	-50	[40]
MGa_2O_4 (M = Mg, Zn)	1385-1400	9.54-10.4	94,600-117,000	-4.0 ~ -27	[41, 42]
$Li_2ZnGe_3O_8$	945	10.3	47,400	-63.9	[43]
$ZnLi_{2/3}Ti_{4/3}O_4$	1075	20.6	106,700	-48	[44]
Zn_2SnO_4	975	9.3	62,000	-50	[45]
$Li_2ATi_3O_8$ (A = Mg, Zn, Co, Ni)	1060-1075	25.6-28.9	2,600-72,000	-11.3 ~ 7.4	[46-48]
$xLi_{4/3}Ti_{5/3}O_4$-(1-x)Mg_2TiO_4 (x = 0.75)	1060	27.1	55,000	2.9	This work